Heat release and high-temperature gas effects in shock/shear-layer interaction

By R. C. Tritarelli AND L. Kleiser

Institute of Fluid Dynamics, ETH Zurich, 8092 Zurich, Switzerland

The interaction of a steady oblique shock wave with a planar shear layer is analysed, including the effect of heat addition and variable heat capacity ratios across the shock. The investigation is performed in the fast-reaction limit, where the shock wave and the following chemical reaction zone are considered as a single discontinuity, neglecting the induction zone between the shock wave and the reaction zone. The high-temperature gas effects, such as the activation of vibrational degrees of freedom, are incorporated using a two-γ shock jump relation and are described using a harmonic oscillator model. An ordinary differential equation governing the shock angle across the shear layer is derived by making use of the Moeckel-Whitham approximation. Hence the result for the shock angle variation across the shear layer can be interpreted as an extension of the Moeckel-Whitham theory for detonation waves with a variable heat capacity ratio across the shock. Possible implications of the shock angle variation on the shock-induced vorticity are discussed.

1. Introduction

As the growth rate of shear layers decreases with increasing convective Mach number (Papamoschou *et al.* [1]), scramjets (supersonic combustion ramjets) require mixing enhancement techniques in order to achieve efficient mixing and combustion. This need is emphasised by the reduction of growth rates in reacting shear layers compared to their non-reactive counterparts, see Mahle [2]. Shock/shear-layer interaction (SSLI) is of great interest as mixing enhancement technique in supersonic combustion systems [3]. First analytical investigations of SSLI were made by Moeckel [4] who derived an ordinary differential equation governing the angle of the propagating shock across the shear layer. The assumption was made that multiply reflected waves can be neglected. Later on Whitham [5] discovered that his characteristic rule is equivalent to neglecting multiply reflected waves as done by Moeckel [4]. Hence this approximation is termed Moeckel-Whitham approximation in the remainder of our study. By making use of this approximation, Buttsworth [6] studied the vorticity production of the SSLI. It was shown that vorticity is produced if the density gradient and velocity gradient of the shear layer were in the same direction. Similar to Moeckel [4] and Whitham [5], he derived his results based on the classical oblique shock wave equations for a perfect gas and adiabatic conditions.

For several applications in supersonic combustion the heat release associated with the shock cannot be neglected and the thermodynamic state across the shock may change from vibrationally frozen to vibrationally excited. Hence the assumption of con-

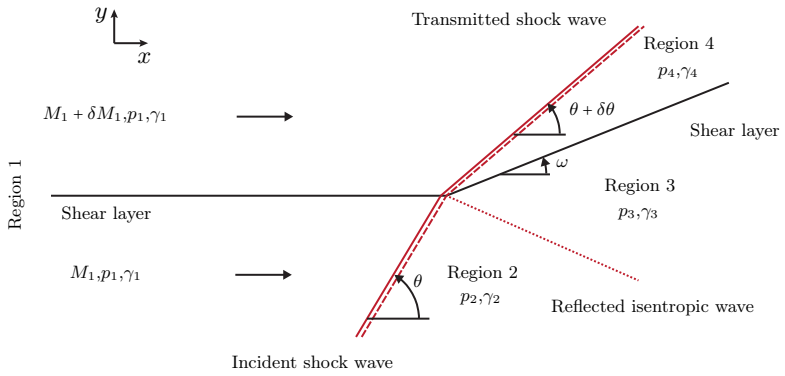

FIGURE 1. Schematic of the shock/shear-layer interaction.

stant specific heat capacity ratios γ and adiabatic conditions across the shock may be too restrictive.

In the present study these restrictions shall be alleviated, and the effect of heat addition and vibrational activation shall be included in the study of SSLI. The equation for the variation of the shock angle across the shear layer will be derived by making use of the two-γ shock jump equations (Li *et al.* [7], Bartlmä [8]). The derived equation can be seen as an extension of the Moeckel-Whitham theory to detonation waves. In a first approximation, the shock wave and the following reaction zone are considered as a single discontinuity, neglecting the induction zone between shock wave and reaction zone, i.e. equilibrium conditions are assumed. This treatment in the fast-reaction limit is permissible as long as the length scale of the induction zone δ_{ind} is negligible compared to the length scale of the shear layer l, i.e. $\delta_{\mathrm{ind}} \ll l$. A schematic of the SSLI is depicted in Fig. 1.

The remainder of this paper is structured as follows. In section 2, the governing equations across the oblique shock wave, i.e. the two-γ shock jump equations, are presented and discussed with respect to the possible impact on the SSLI vorticity production. In the following section 3 the equation governing the shock angle variation due to pre-shock Mach number non-uniformities is derived and analysed regarding the impact of heat addition and variable heat capacity ratios. In section 4 the possible impact of the shock curvature on the shock-induced vorticity is discussed; a conclusion and an outlook for future studies are presented.

2. Governing equations

2.1. *Two-γ shock jump equations*

The governing equations for oblique shock waves are covered in many textbooks and were the starting point for the derivations of Moeckel [4], Whitham [5] and Buttsworth [6]. In classical textbooks the development of the shock jump relations does not take into account varying specific heat capacity ratios γ between the pre-shock and post-shock state, as present for vibrationally active molecules, such as nitrogen and oxygen. The present chapter presents the two-γ shock jump relations with heat addition, which forms the starting point for the extension of the Moeckel-Whitham theory in the subsequent chapter. The two-γ shock jump relations are discussed in the works by Li *et al.* [7] and Bartlmä [8]. The equations for oblique shock waves can directly be obtained from the

normal shock jump equations and hence the equations for a normal shock are stated first. The governing equations of mass, momentum and energy across a normal shock wave can be written as follows

$$\rho_1 u_{n,1} = \rho_2 u_{n,2} \tag{2.1}$$

$$p_1 + \rho_1 u_{n,1}^2 = p_2 + \rho_2 u_{n,2}^2 \tag{2.2}$$

$$h_1 + \frac{1}{2} u_{n,1}^2 + q = h_2 + \frac{1}{2} u_{n,2}^2 \tag{2.3}$$

where ρ, u_n, p and h are respectively the density, normal velocity, pressure and enthalpy. The conditions 1 and 2 refer to the pre-shock and post-shock state, respectively. q is the heat addition per unit of mass. In the present analysis, we are considering a thermally perfect but not calorically perfect gas, which satisfies the following thermodynamic properties

$$h_j = h_j(T) = c_{p,j}(T_j)\, T_j \tag{2.4}$$

$$a_j^2 = \gamma_j p_j / \rho_j \tag{2.5}$$

$$p_j = \rho_j R_j T_j \tag{2.6}$$

$$\gamma_j = c_{p,j}/c_{v,j} \quad \text{with} \quad c_{p,j} = c_{v,j} + R_j \tag{2.7}$$

where $j \in \{1, 2\}$ and a_j, γ_j, $c_{p,j}$, $c_{v,j}$ and R_j are the speed of sound, heat capacity ratio, isobaric and isochoric heat capacity as well as the mass-specific gas constant, respectively. The functional temperature dependence of $c_{p,j}(T)$ will be discussed in the following section 2.2. Note that in general the equilibrium speed of sound for a non-perfect gas is given as

$$a^2 = \gamma R T \, \frac{1 + (1/p)(\partial e/\partial v)_T}{1 - \rho(\partial h/\partial p)_T}, \tag{2.8}$$

where e and v are the internal energy and specific volume, respectively (Anderson [9]). Since we are considering a thermally perfect gas where $h_j = h_j(T)$, Eq. (2.8) reduces to Eq. (2.5). Equations (2.4) and (2.5) are not directly applicable to SSLI with a change in γ due to dissociation, as we would have $h = h(T, p)$ and hence $\gamma = \gamma(T, p)$ and a would need to be computed following Eq. (2.8).

From the governing equations, the shock jump relations can be derived (Li *et al.* [7]). The pressure variation across a shock reads

$$f_1^{2\gamma}(M_1, \theta, \gamma_1, \gamma_2, \bar{q}) := \frac{p_2}{p_1} = \frac{(1+\beta)\gamma_1 M_{n,1}^2 - \gamma_2 \beta + 1}{\gamma_2 + 1}, \tag{2.9}$$

with $M_{n,1}$ being the pre-shock normal Mach number defined as $M_{n,1} := M_1 \sin\theta$. θ refers to the shock angle and β is an auxiliary variable defined as

$$\beta := \sqrt{1 - \frac{2(\gamma_2^2 - 1) M_{n,1}^2 (\bar{q} + \eta)}{(M_{n,1}^2 - \Gamma)^2}}, \tag{2.10}$$

where we made use of

$$\eta := \frac{\Gamma - 1}{(\gamma_1 - 1)(\gamma_2 - 1)}, \qquad \text{and} \qquad \Gamma := \frac{\gamma_2}{\gamma_1}. \tag{2.11}$$

For the case of an adiabatic shock and a constant heat capacity ratio β reduces to $\beta = 1$ and the shock jump equations reduce to the Rankine-Hugoniot relations. The heat

addition q was normalised by the pre-shock speed of sound $\bar{q} := q/a_1^2$. The pressure ratio was abbreviated as $f_1^{2\gamma}$, where the superscript 2γ indicates that the pre-shock and post-shock heat capacity ratios are assumed to be a priori known constants, i.e. γ_1 and γ_2 are not functions of M or θ, respectively. This shall be contrasted to f_1^{HO}, which will be defined in the subsequent section (the superscript HO stands for harmonic oscillator). In that case, γ_2 will be a solution of the governing and constitutive equations and hence depend on M and θ.
The density ratio ϵ can be computed as

$$\epsilon^{2\gamma}(M_1, \theta, \gamma_1, \gamma_2, \bar{q}) := \frac{\rho_1}{\rho_2} = 1 - \frac{1+\beta}{\gamma_2+1}(1 - \Gamma/M_{n,1}^2). \tag{2.12}$$

The ratio of speeds of sound is given by

$$\frac{a_2^2}{a_1^2} = \frac{\gamma_1}{\gamma_2}\frac{p_2}{p_1}\frac{\rho_1}{\rho_2}, \tag{2.13}$$

and hence the temperature ratio follows immediately as

$$\frac{T_2}{T_1} = \frac{\gamma_1 R_1}{\gamma_2 R_2}\frac{a_2^2}{a_1^2}. \tag{2.14}$$

The flow deflection angle ω (see Fig. 1) can be evaluated as

$$\begin{aligned} \omega &= \theta - \arctan\left[\frac{\gamma_2-\beta}{\gamma_2+1}\tan\theta + \frac{2\,\Gamma\,(1+\beta)}{(\gamma_2+1)\,M_1^2\,\sin(2\,\theta)}\right], \\ \omega &=: f_2^{2\gamma}\left(M_1, \theta, \gamma_1, \gamma_2, \bar{q}\right), \end{aligned} \tag{2.15}$$

(Li *et al.* [7]) and the post-shock Mach number is given by

$$M_2^2 = \left[M_{1,n}^2\left(\left(\frac{\rho_1}{\rho_2}\right)^2 - 1\right) + M_1^2\right]\frac{\gamma_1}{\gamma_2}\frac{p_1}{p_2}\frac{\rho_2}{\rho_1} \tag{2.16}$$

(Bartlmä [8]). Analogous to the case of a normal shock, a critical heat addition for a given shock angle θ exists. The critical normalised heat addition is given by

$$\bar{q}_{\mathrm{crit}}^{2\gamma}(M_1, \theta, \gamma_1, \gamma_2) = \frac{\left(M_{n,1}^2 - \gamma_2/\gamma_1\right)^2}{2\,(\gamma_2^2-1)M_{n,1}^2} - \eta \tag{2.17}$$

(Bartlmä [8]). At critical conditions we have $\beta = 0$. In the remainder the heat addition across an oblique detonation wave will be expressed as fraction of the critical heat addition.

2.2. *Harmonic oscillator model*

In the previous section the pre-shock and post-shock heat capacity ratios were assumed to be a priori known quantities. In the following the temperature dependence of the heat capacity will be described by a simplified model for vibrational excitation, i.e. the harmonic oscillator model [10], which allows to make use of a non-dimensional formulation of the problem. The volumetric heat capacity for a diatomic molecule can be written as

$$c_{v,j}\left(\widetilde{T}_{j,\mathrm{vib}}\right) = R_j\left\{\frac{5}{2} + \left[\frac{1/\left(2\,\widetilde{T}_{j,\mathrm{vib}}\right)}{\sinh\left(1/\left(2\,\widetilde{T}_{j,\mathrm{vib}}\right)\right)}\right]^2\right\}, \tag{2.18}$$

where we made use of the non-dimensional temperature $\widetilde{T}_{\mathrm{vib}} = T/T_{\mathrm{vib}}$ with T_{vib} being a characteristic vibrational temperature of the species under consideration. Characteristic vibrational temperatures of interest for scramjet applications are $T_{\mathrm{vib,O_2}} = 2273\,\mathrm{K}$, $T_{\mathrm{vib,N_2}} = 3395\,\mathrm{K}$, and $T_{\mathrm{vib,H_2}} = 6332\,\mathrm{K}$, see Karl [11]. Obviously from the definition of Eq. (2.18) we obtain that $\gamma_j = \gamma_j(\widetilde{T}_{j,\mathrm{vib}})$.
For the limits of small and large $\widetilde{T}_{\mathrm{vib}}$ one can define $c_{v,\mathrm{di}}$ and $c_{v,\mathrm{vib}}$ as

$$c_{v,\mathrm{di}} \coloneqq \lim_{\widetilde{T}_{\mathrm{vib}}\to 0^+} c_{v,j}(\widetilde{T}_{\mathrm{vib}}) = 5/2\, R_j, \tag{2.19}$$

$$c_{v,\mathrm{vib}} \coloneqq \lim_{\widetilde{T}_{\mathrm{vib}}\to \infty} c_{v,j}(\widetilde{T}_{\mathrm{vib}}) = 7/2\, R_j, \tag{2.20}$$

where $(\cdot)_{\mathrm{di}}$ and $(\cdot)_{\mathrm{vib}}$ refer to a diatomic molecule without and with complete vibrational excitation, respectively. In the same limits we obtain $\gamma_{\mathrm{di}} = 7/5$ and $\gamma_{\mathrm{vib}} = 9/7$.

Once the harmonic oscillator model is used as constitutive relation, the functional dependence of the pressure ratio, the density ratio, etc. across the shock wave are altered. This change in functional dependence is shown exemplary for the pressure ratio, which reads

$$f_1^{\mathrm{HO}}(M_1, \theta, \widetilde{T}_{1,\mathrm{vib}}, \bar{q}) \coloneqq f_1^{2\gamma}(M_1, \theta, \gamma_1(\widetilde{T}_{1,\mathrm{vib}}), \gamma_2(\widetilde{T}_{2,\mathrm{vib}}(M_1, \theta, \widetilde{T}_{1,\mathrm{vib}}, \bar{q})), \bar{q}). \tag{2.21}$$

The normalised post-shock temperature $\widetilde{T}_{2,\mathrm{vib}}$ and the heat capacity ratio γ_2 can be obtained by solving simultaneously Eq. (2.14) and Eq. (2.18). Note that

$$\frac{\partial f_1^{2\gamma}}{\partial M} \neq \frac{\partial f_1^{\mathrm{HO}}}{\partial M}, \tag{2.22}$$

as for f_1^{HO} a change in M induces a change in γ_2, whereas it does not for $f_1^{2\gamma}$. This formal difference is of importance for the application of the Moeckel-Whitham theory to oblique detonation waves in the following chapters. Note that for vibrational activation across a shock wave we have $\gamma_2 < \gamma_1$, and hence $\eta < 0$. From Eq. (2.10) it can be concluded that the effect of vibrational activation is similar to a heat sink across the shock wave. This heat sink will result in a higher density ratio across the shock wave and thereupon increase the vorticity production due to SSLI. The impact of the variable γ on the density ratio will be analysed below.

2.3. *Effect of vibrational activation on the amplification factor $\mathcal{Z}_\epsilon$*

In order to study the impact of variable heat capacity ratios on the vorticity production, it is of importance to study the density ratio across a shock wave as a function of the non-dimensional pre-shock temperature $\widetilde{T}_{1,\mathrm{vib}}$, as the vorticity production is a function of the density ratio across the shock. In the following sections the vorticity production due to shock wave curvature will be discussed. It will be seen that this part of the vorticity production is proportional to $\mathcal{Z}_\epsilon$, which is defined as

$$\mathcal{Z}_\epsilon \coloneqq \frac{(1-\epsilon)^2}{\epsilon}. \tag{2.23}$$

In order to highlight the impact of variable heat capacity ratios, we will investigate the normalised amplification factor defined as

$$\mathcal{Z}_{\epsilon,\mathrm{di}}(M_1, \theta, \widetilde{T}_{1,\mathrm{vib}}, \bar{q}) \coloneqq \frac{\mathcal{Z}_\epsilon^{\mathrm{HO}}(M, \theta, \widetilde{T}_{1,\mathrm{vib}}, \bar{q})}{\lim\limits_{\widetilde{T}_{1,\mathrm{vib}}\to 0^+} \mathcal{Z}_\epsilon^{\mathrm{HO}}(M, \theta, \widetilde{T}_{1,\mathrm{vib}}, \bar{q})}, \tag{2.24}$$

which is the ratio of the amplification factor of a two-γ shock to that of a single-γ shock with frozen vibrational motion. Similar to $\mathcal{Z}_{\epsilon,\mathrm{di}}$, $\mathcal{Z}_{\epsilon,\mathrm{vib}}$ can be defined by computing in the denominator of Eq. (2.24) a limit of $\widetilde{T}_{1,\mathrm{vib}}$ tending to infinity instead of computing a limit tending to zero. We will analyse $\mathcal{Z}_{\epsilon,\mathrm{di}}$ and $\mathcal{Z}_{\epsilon,\mathrm{vib}}$ for constant incident shock angles. In the presented results, we make use of the following parametrisation of the heat addition across the oblique detonation wave

$$\alpha_\theta := \frac{\bar{q}}{\bar{q}^{2\gamma}_{\mathrm{crit}}(M_1, \theta, \gamma_{\mathrm{di}}, \gamma_{\mathrm{di}})}. \tag{2.25}$$

Hence, $\alpha_{\pi/2}$ indicates that the heat addition has been normalised with the critical heat addition for a normal shock.

It can be seen from Figs. 2 and 3 that the density jump and therefore the amplification factor $\mathcal{Z}_\epsilon$ are increased due to vibrational activation. This effect is most pronounced at intermediate temperatures, where the vibrational activation acts like a heat sink and reduces the post-shock temperature and increases the post-shock density. We can observe from the right part of Figs. 2 and 3 that the impact of vibrational activation on $\mathcal{Z}_\epsilon$ is more important for detonation waves than for adiabatic shock waves as $\mathcal{Z}_\epsilon$ is increasing with $\alpha_{\pi/2}$. Comparing Figs. 2 and 3, both analysing $\mathcal{Z}_\epsilon$ but making use of different normalisations, one can observe that interpretations have to be made with care when discussing trends regarding Mach number and heat addition. In the left part of Fig. 3 one can recognise that the impact of vibrational activation reduces with increasing Mach number. This trend holds true when $\mathcal{Z}_\epsilon$ is normalised with the high-temperature limit. This observation is expected, as the ratio of the pre-shock thermal to the pre-shock kinetic energy reduces with increasing Mach number, such that in the hypersonic limit the density ratio depends exclusively on post-shock quantities (Hayes and Probstein [12]), which means

$$\lim_{M_{n,1}\to\infty} \epsilon = \frac{\gamma_2 - 1}{\gamma_2 + 1}. \tag{2.26}$$

From this it can be concluded that the maximum of $\mathcal{Z}_{\epsilon,\mathrm{vib}}$ tends to unity as the normal Mach number tends to infinity, which is observed in Fig. 3. On the other hand a non-monotonic behaviour of the maximum of $\mathcal{Z}_{\epsilon,\mathrm{di}}$ with respect to Mach number is observed in Fig. 2. Thus a conclusion regarding the effect of Mach number on the importance of vibrational activation in $\mathcal{Z}_\epsilon$ is difficult and depends on the particular normalisation of $\mathcal{Z}_\epsilon$. On the contrary, the trend regarding $\alpha_{\pi/2}$ is the same for $\mathcal{Z}_{\epsilon,\mathrm{di}}$ and $\mathcal{Z}_{\epsilon,\mathrm{vib}}$, and we can conclude that the importance of including the vibrational activation in the computation of $\mathcal{Z}_\epsilon$ increases with increasing heat addition. The augmentation of $\mathcal{Z}_\epsilon$ due to vibrational activation can engender an increase of vorticity production due to SSLI. In order to assess this vorticity production, the impact of vibrational activation on the shock curvature needs to be analysed. To this end we derive an extension of the Moeckel-Whitham theory in the following section.

3. Extension of the Moeckel-Whitham theory

3.1. *Shock angle variation for a non-uniform pre-shock Mach number distribution, under the restriction* $\gamma_2 = \gamma_3 = \gamma_4$

In order to derive the variation of the shock angle through a shear layer of varying incoming Mach number, the assumptions are made that the incoming flow is parallel and

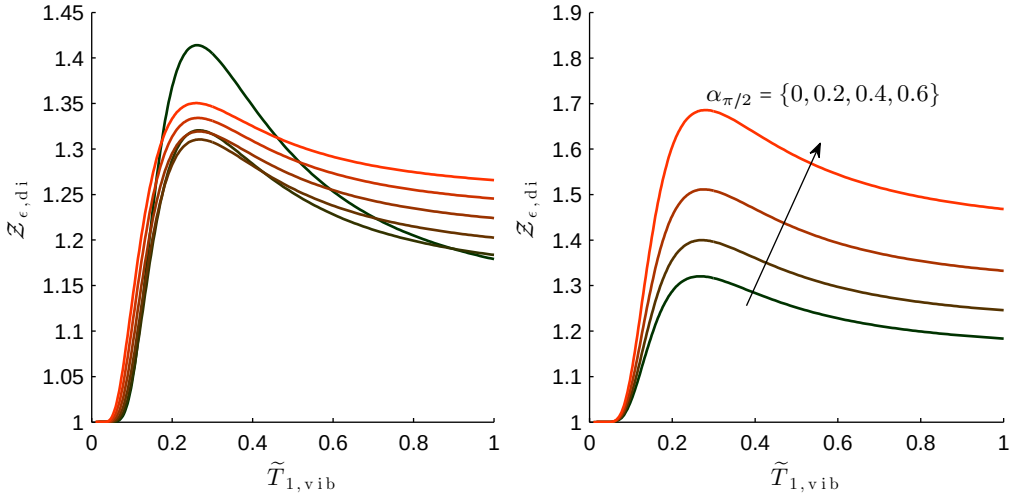

FIGURE 2. Normalised amplification factor $\mathcal{Z}_{\epsilon,\mathrm{di}}$ for (left) adiabatic conditions and variable Mach numbers $M_{n,1} = \{1.25, 1.5, \ldots, 2.5\}$ from black to red and (right) constant $M_n = 1.5$ and different levels of heat addition $\alpha_{\pi/2}$.

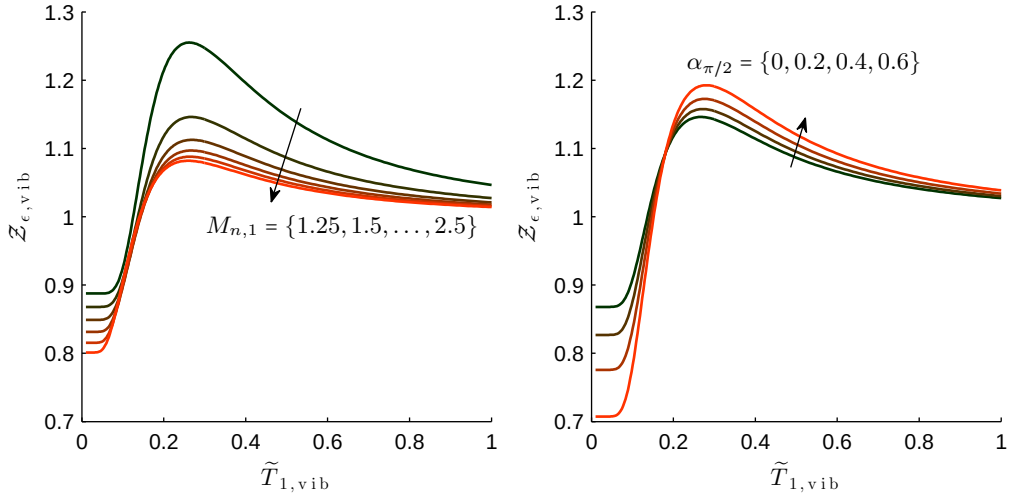

FIGURE 3. Normalised amplification factor $\mathcal{Z}_{\epsilon,\mathrm{vib}}$ for (left) adiabatic conditions and variable Mach numbers and (right) constant Mach number $M_n = 1.5$ and different levels of heat addition $\alpha_{\pi/2}$.

that pressure gradients are negligible. The post-shock state is assumed to remain supersonic, and the pre-shock Mach number is assumed to vary continuously, such that the Mach number variation can be split into a sequence of infinitesimal Mach number changes δM_1, where δ indicates small changes. In contrast to Buttsworth [6], no adiabatic conditions are assumed and the heat capacity ratio is allowed to change throughout the shock wave. The situation is sketched schematically in Fig. 1. The pre-shock heat capacity ratio γ_1 is assumed to be constant, i.e. $\gamma_1 \neq \gamma_1(y)$. Additionally we will assume $\gamma_2 = \gamma_3 = \gamma_4$, but we will allow a change of heat capacity ratios across the shock, i.e. $\gamma_1 \neq \gamma_2$. The incident shock wave will be partially transmitted and partially

reflected. Due to the small Mach number change, the reflected wave can be assumed to be an isentropic (expansion or compression) wave. The nature of the reflected isentropic wave depends on the combination of Mach number, shock angle, heat addition and non-dimensional temperature. The flow across the dividing streamline will be parallel and have the same pressure. Hence the conditions across the slip line are

$$p_3 = p_4, \tag{3.1}$$

$$\omega_3 = \omega_4, \tag{3.2}$$

with $p_4 = p_2 + \delta p_4$ and $p_3 = p_2 + \delta p_3$. From these conditions we can derive the change in shock angle $\delta\theta$ due to a change in Mach number δM_1. We are following the lines of the derivation by Buttsworth [6], but we are starting from the two-γ shock jump relations instead of starting from the classical Rankine-Hugoniot relations. Equation (2.9) governing the pressure jump across the shock can be linearized for small normal Mach number variations $\delta M_{n,1}$, resulting in

$$\frac{\delta p_4}{p_1} = \frac{1}{\gamma_2 + 1}\left[2\,\gamma_1\, M_{n,1}(1+\beta) + \gamma_1\, M_{n,1}^2\beta' - \gamma_2\,\beta'\right]\delta M_{n,1}, \tag{3.3}$$

where $\delta M_{n,1}$ can be written as

$$\delta M_{n,1} = \delta M_1 \sin\theta + \delta\theta_1 M_1 \cos\theta \tag{3.4}$$

and $\beta' \coloneqq \frac{d\beta}{dM_{n,1}}$. The following useful relations can be defined

$$\beta_{M_1} = \frac{\partial\beta}{\partial M_1} = \frac{d\beta}{dM_{n,1}}\sin\theta = \beta'\,\sin\theta, \tag{3.5}$$

$$\beta_\theta = \frac{\partial\beta}{\partial\theta} = \frac{d\beta}{dM_{n,1}}\,M_1\,\cos\theta = \beta'\,M_1\,\cos\theta, \tag{3.6}$$

$$\beta' = \frac{\left(1-\beta^2\right)\left(M_{n,1}^2+\Gamma\right)}{\beta M_{n,1}\left(M_{n,1}^2-\Gamma\right)} \tag{3.7}$$

(Li *et al.* [13]). Note that as $\bar{q}$ tends to $\bar{q}_{\mathrm{crit}}$, β tends to zero and β' tends to infinity. In the present analysis the heat addition will be limited to sub-critical conditions.

In a similar way Eq. (2.15), describing the flow deflection angle, can be written after neglecting higher order terms as

$$\mathcal{A}\,\delta M_1 + \mathcal{B}\,\delta\theta + \mathcal{C}\,\delta\omega = 0. \tag{3.8}$$

The terms $\mathcal{A}$, $\mathcal{B}$ and $\mathcal{C}$ can be derived to be

$$\mathcal{A} = M_1(\gamma_2+1)\cos\theta\,\sin\theta\left[M_1^3\beta_{M_1}\sin^2\theta - \Gamma\,\beta_{M_1}M_1 + 2\,\Gamma(1+\beta)\right], \tag{3.9}$$

$$\begin{aligned}\mathcal{B} = {}& (\beta+1)\sin^2\theta\,\left(\gamma_2+1+(\beta-1-2\,\gamma_2)\sin^2\theta\right)\,M_1^4\\ &+\Gamma\,(\beta+1)\left(\gamma_2+1-2\,(\beta+1)\sin^2\theta\right)\,M_1^2+\Gamma^2\,(1+\beta)^2\\ &+\beta_\theta\,(\gamma_2+1)\,\sin\theta\,\cos\theta\,(M_1^4\sin^2\theta-\Gamma\,M_1^2),\end{aligned} \tag{3.10}$$

and

$$\begin{aligned}\mathcal{C} = {}& \sin^2\theta\,\left((1-\beta^2+2\,\gamma_2\,(\beta+1))\,\sin^2\theta-(\gamma_2+1)^2\right)\,M_1^4\\ &-2\,\Gamma\,(1+\beta)\,(\gamma_2-\beta)\,M_1^2\,\sin^2\theta-\Gamma^2\,(\beta+1)^2.\end{aligned} \tag{3.11}$$

For the case $\beta = 1$, $\beta' = 0$, and $\Gamma = 1$ we obtain the equations derived by Buttsworth [6].

Combining the pressure change across the reflected isentropic wave with the requirement of matched flow direction, one obtains

$$\frac{\delta p_3}{p_2} = -\frac{\gamma_2 M_2^2}{(M_2^2-1)^{1/2}}\delta\omega. \tag{3.12}$$

The previous equation can be abbreviated using the following definition

$$f_3^{2\gamma}(M_1,\theta,\gamma_1,\gamma_2,\bar{q}) := \frac{\gamma_2 M_2^2}{(M_2^2-1)^{1/2}}. \tag{3.13}$$

The condition of matched pressure implies that

$$\frac{\delta p_4}{p_1} = \frac{\delta p_3}{p_2}\frac{p_2}{p_1}. \tag{3.14}$$

Combining Eqs. (3.3), (3.12) and (3.14) results in

$$\begin{aligned}&[2\,M_{n,1}(1+\beta) + M_{n,1}^2\beta' - \Gamma\,\beta']\delta M_{n,1}\\ &\quad + \frac{M_2^2}{(M_2^2-1)^{1/2}}\left[(1+\beta)\,\gamma_2\,M_{n,1}^2 - \Gamma\,\gamma_2\,\beta + \Gamma\right]\delta\omega = 0.\end{aligned} \tag{3.15}$$

Equations (3.15) and (3.8) can be used to eliminate $\delta\omega$, which results in an equation of the form

$$\frac{\delta\theta}{\delta M} = -\frac{\frac{1}{f_1^{2\gamma}}\frac{\partial f_1^{2\gamma}}{\partial M} + f_3^{2\gamma}\frac{\partial f_2^{2\gamma}}{\partial M}}{\frac{1}{f_1^{2\gamma}}\frac{\partial f_1^{2\gamma}}{\partial \theta} + f_3^{2\gamma}\frac{\partial f_2^{2\gamma}}{\partial \theta}}. \tag{3.16}$$

Equation (3.16) describes the variation of the shock angle due to a single and isolated Mach number jump δM. By neglecting multiple reflections we can replace $\delta\theta/\delta M$ by $d\theta/dM$ and obtain a nonlinear ODE which describes the variation of the shock angle through the shear layer

$$f^{2\gamma}(M,\theta,\gamma_1,\gamma_2,\bar{q}) := \frac{d\theta}{dM} = -\frac{\frac{1}{f_1^{2\gamma}}\frac{\partial f_1^{2\gamma}}{\partial M} + f_3^{2\gamma}\frac{\partial f_2^{2\gamma}}{\partial M}}{\frac{1}{f_1^{2\gamma}}\frac{\partial f_1^{2\gamma}}{\partial \theta} + f_3^{2\gamma}\frac{\partial f_2^{2\gamma}}{\partial \theta}}, \tag{3.17}$$

where $f_1^{2\gamma}$, $f_2^{2\gamma}$, and $f_3^{2\gamma}$ were defined previously. $\frac{\partial f_1^{2\gamma}}{\partial M}$ and $\frac{\partial f_1^{2\gamma}}{\partial \theta}$ can be obtained from Eqs. (3.3) and (3.4), and we have

$$\frac{\partial f_2^{2\gamma}}{\partial M} = -\mathcal{A}/\mathcal{C}, \tag{3.18}$$

$$\frac{\partial f_2^{2\gamma}}{\partial \theta} = -\mathcal{B}/\mathcal{C}. \tag{3.19}$$

Note that similar to the definition of f_1^{HO}(Eq. (2.21)) we can define f^{HO}. Equation (3.17) is identical to the equations given by Moeckel [4] and Whitham [5], however the functions $f_1^{2\gamma}$, $f_2^{2\gamma}$, $f_3^{2\gamma}$, and their derivatives are different as we took the two-γ shock relations as a starting point for the derivation. As discussed by Whitham [5], neglecting multiply reflected waves is identical to applying his characteristic rule. The assumption of neglecting secondary waves and other multiply reflected waves in the Moeckel-Whitham theory is analogous to the assumptions underlying the Chester-Chisnell-Whitham (CCW) theory, see [5, 14].

3.2. *Shock angle variation for a non-uniform pre-shock Mach number distribution, under the restriction* $\gamma_2 = \gamma_3$

In the previous section we computed the shock angle variation for a non-uniform pre-shock Mach number distribution under the restriction that $\gamma_2 = \gamma_3 = \gamma_4$. If we alleviate this restriction we can compute the shock angle variation in a similar manner as

$$g^{\mathrm{HO}}(M_1, \theta, \widetilde{T}_{1,\mathrm{vib}}, \bar{q}) := \frac{d\theta}{dM} = -\frac{\frac{1}{f_1^{\mathrm{HO}}}\frac{\partial f_1^{\mathrm{HO}}}{\partial M} + f_3^{\mathrm{HO}}\frac{\partial f_2^{\mathrm{HO}}}{\partial M}}{\frac{1}{f_1^{\mathrm{HO}}}\frac{\partial f_1^{\mathrm{HO}}}{\partial \theta} + f_3^{\mathrm{HO}}\frac{\partial f_2^{\mathrm{HO}}}{\partial \theta}}. \tag{3.20}$$

The assumption that $\gamma_2 = \gamma_3$ is still made, i.e. the heat capacity is assumed to be constant across the isentropic wave. It can be observed that Eqs. (3.17) and (3.20) are identical after replacing $f_k^{2\gamma}$ by f_k^{HO} for $k \in \{1, 2, 3\}$. It should be noted that $g^{\mathrm{HO}} \neq f^{\mathrm{HO}}$ and that $g^{2\gamma}$ does not exist. Additionally it should be noted that in Eq. 3.17 all the terms were expressed in an analytical form. In the present study we did not express all the terms of Eq. 3.20 analytically. The partial differentials in the formulation of g^{HO} were hence evaluated numerically. Comparisons of f^{HO} to g^{HO} will be presented in the following section.

3.3. *Numerical evaluation of the shock angle variation*

In the previous sections, we saw that $\mathcal{Z}_\epsilon$ was increased due to vibrational activation (Figs. 2 and 3). In the current section the shock angle variation will be analysed with respect to its variation for different non-dimensional temperatures $\widetilde{T}_{1,\mathrm{vib}}$. To this end we will analyse the shock angle variation $\frac{d\theta}{dM}$ normalised with the diatomic limit, i.e.

$$\left.\frac{d\theta}{dM}\right|_{\mathrm{di}} := \frac{\frac{d\theta}{dM}(M, \theta, \widetilde{T}_{1,\mathrm{vib}}, \bar{q})}{\lim\limits_{\widetilde{T}_{1,\mathrm{vib}} \to 0^+} \frac{d\theta}{dM}(M, \theta, \widetilde{T}_{1,\mathrm{vib}}, \bar{q})}. \tag{3.21}$$

The normalised shock angle variation $\left.\frac{d\theta}{dM}\right|_{\mathrm{di}}$ can be evaluated using either f^{HO} or g^{HO} for the shock angle variation $\frac{d\theta}{dM}$. In the left part of Fig. 4 we observe that due to vibrational activation the shock angle variation is reduced for the largest part of the temperature range. At low temperatures a small increase can be observed for g^{HO} or more precisely for $\left.\frac{d\theta}{dM}\right|_{\mathrm{di}}$ based on g^{HO}. The minimum of $\left.\frac{d\theta}{dM}\right|_{\mathrm{di}}$ based on f^{HO} and g^{HO} is observed for an intermediate temperature range around $\widetilde{T}_{1,\mathrm{vib}} \approx 0.25$. For the present combination of Mach number and shock angle θ, g^{HO} is larger than f^{HO}. This observation does not hold true in general. The ratio of g^{HO} to f^{HO} depends on the combination of M and θ and depends most likely on the fact that the reflected isentropic wave in Fig. 1 can be a compression wave or an expansion wave. The ratio of g^{HO} to f^{HO} is expected to be a function of the type and strength of the reflected isentropic wave. This is an open question, which will be analysed in future studies. For both plots in Fig. 4 a constant incident shock angle θ was assumed. The right part of Fig. 4 shows the effect of adding heat across the shock wave. The impact of vibrational activation on $\left.\frac{d\theta}{dM}\right|_{\mathrm{di}}$ is more important for a detonation wave than for a shock wave if the shock angle variation is normalised with the diatomic limit.

From the precedent results a reduction of vorticity production due to vibrational activation could be expected, as the reduction of the shock angle variation due to vibrational activation is equivalent to a reduction of the shock curvature. The question rises whether the effect of the reduced curvature or the effect of the increased amplification factor $\mathcal{Z}_\epsilon$ is dominant.

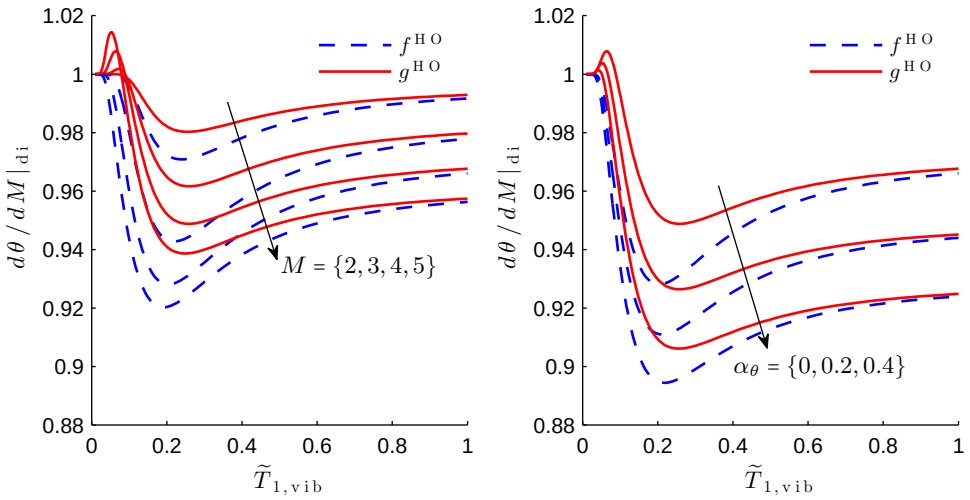

FIGURE 4. Shock angle variation $\frac{d\theta}{dM}$ for (left) adiabatic conditions with different Mach numbers and (right) constant Mach number $M = 4$ for different levels of heat addition α_θ. The incident shock angle in both cases is $\theta = \pi/4$.

4. Possible implications of vibrational activation on shock-wave-induced vorticity and conlusions

In the previous sections we have seen two counteracting trends affecting the vorticity production, i.e. the increase of the amplification factor $\mathcal{Z}_\epsilon$ and the decrease of the shock angle variation due to vibrational activation. In order to study the vorticity production across a curved shock in a non-uniform flow we can make use of Hayes' vorticity equation [15]. This is a dynamical relation, which can also be applied to detonation waves. As shown by Buttsworth [6], for a planar problem, Hayes' vorticity equation can be written as

$$\begin{aligned}\zeta_2 = &\left[\mathcal{Z}\frac{d\theta}{dM} + 2\left(\epsilon - 1\right)\,\sin^2\theta - \epsilon\sin^2\theta - \frac{1}{\epsilon}\cos^2\theta\right]\frac{du_1}{dy} \\ &+ \left[\mathcal{Z}\frac{d\theta}{dM} + 2\left(\epsilon - 1\right)\,\sin^2\theta\right]\frac{u_1}{2\rho_1}\frac{d\rho_1}{dy},\end{aligned} \tag{4.1}$$

where ζ_2 is the post-shock vorticity, $\mathcal{Z}$ is defined as

$$\mathcal{Z} := \frac{(1-\epsilon)^2}{\epsilon}\,M_1\,\sin\theta\,\cos\theta = \mathcal{Z}_\epsilon\,M_1\,\sin\theta\,\cos\theta, \tag{4.2}$$

and $\mathcal{Z}_\epsilon$ was already defined in Eq. (2.23) and discussed in previous sections. From Eq. (4.1) we can see that the vorticity production due to the curvature of the shock is proportional to $\mathcal{Z}\frac{d\theta}{dM}$. Based on the results of the present study we observe that the vorticity is enhanced due to vibrational activation if considering constant incident shock angles, as the increase in $\mathcal{Z}_\epsilon$ (Fig. 2) is larger than the reduction of shock angle variation (Fig. 4).

In conclusion, we derived an equation governing the shock angle variation $d\theta/dM$ for a thermally perfect (but not calorically perfect) gas. We observed that $\mathcal{Z}_\epsilon$ is increased due to the vibrational activation whereas $|d\theta/dM|$ is reduced when considering constant

incoming shock angles. Hence, we observe two counteracting trends influencing the vorticity production due to shock curvature. However, the impact of vibrational activation is much larger for $\mathcal{Z}_\epsilon$ than for $d\theta/dM$. We can conclude that vibrational activation increases the vorticity production due to shock curvature if considering constant incident shock angles for all non-dimensional temperatures $\widetilde{T}_{1,\mathrm{vib}}$. Future investigations shall analyse whether this trend holds true if the deflection angle is kept constant for all non-dimensional temperatures $\widetilde{T}_{1,\mathrm{vib}}$. Additionally, we shall analyse the complete vorticity production across the shock wave and compare the ratio of the vorticity production due to shock curvature to the total vorticity production. Furthermore, the (M,θ)-phase-space will be classified regarding the nature of the reflected isentropic wave and we will make use of this classification in order to discuss the ratio of g^{HO} to f^{HO}.

References

[1] PAPAMOSCHOU, D. AND ROSHKO, A. (1988). The compressible turbulent shear layer: an experimental study. *J. Fluid Mech.*, **197**, 453–477.

[2] MAHLE, I., FOYSI, H., SARKAR, S. AND FRIEDRICH, R. (2007). On the turbulence structure in inert and reacting compressible mixing layers. *J. Fluid Mech.*, **593**, 171–180.

[3] SEINER, J. M., DASH, S. M. AND KENZAKOWSKI, D. C. (2001). Historical survey on enhanced mixing in scramjet engines. *J. Prop. Power*, **17**(6), 1273–1286.

[4] MOECKEL, W. E. (1952). Interaction of oblique shock waves with regions of variable pressure, entropy, and energy. *NACA Technical Note 2725*.

[5] WHITHAM, G. B. (1958). On the propagation of shock waves through regions of non-uniform area or flow. *J. Fluid Mech.*, **4**, 337–360.

[6] BUTTSWORTH, D. R. (1996). Interaction of oblique shock waves and planar mixing regions. *J. Fluid Mech.*, **306**, 43–57.

[7] LI, H., BEN-DOR, G. AND GRÖNIG, H. (1997). Analytical study of the oblique reflection of detonation waves. *AIAA J.*, **35**(11), 1712–1720.

[8] BARTLMÄ, F. (1967). Schiefe Reaktionsfronten. *DLR Forschungsbericht 67-73*.

[9] ANDERSON, J. D. (1982). *Modern Compressible Flow*. McGraw-Hill

[10] VINCENTI, W. G. AND KRUGER, C. H. (1965). *Introduction to Physical Gas Dynamics*. Wiley.

[11] KARL, S. (2011). *Numerical Investigation of a Generic Scramjet Configuration.* Ph.D. thesis, TU Dresden.

[12] HAYES, W. D. AND PROBSTEIN R. F. (1959). *Hypersonic Flow Theory*. Academic Press.

[13] LI, H. AND BEN-DOR, G. (1998). A Modified CCW Theory for Detonation Waves. *Combust. Flame*, **113**(1-2), 1–12.

[14] CHISNELL, R. F. (1957). The motion of a shock wave in a channel, with applications to cylindrical and spherical shock waves. *J. Fluid Mech.*, **2**(3), 286–298.

[15] HAYES, W. D. (1957). The vorticity jump across a gasdynamic discontinuity. *J. Fluid Mech.*, **2**(6), 595–600.